

Fast-Neutron Capture Cross Section of Ni<sup>64</sup>†

H. A. GRENCH

*Lockheed Palo Alto Research Laboratories, Palo Alto, California*

(Received 30 July 1965)

The fast-neutron capture cross section of Ni<sup>64</sup> has been measured by the activation technique at 18 neutron energies between approximately 0.2 and 2.0 MeV. The measurements were made relative to the Au<sup>197</sup>(*n,γ*)Au<sup>198</sup> cross section. The results have been interpreted in terms of the statistical theory of nuclear reactions and the Fermi-gas level-spacing model. A good fit to the data was obtained with the adjustment of a single free parameter. A value of 0.34 eV was obtained for the average radiation width of the  $\frac{1}{2}^+$  levels in Ni<sup>66</sup> at the neutron binding energy.

## INTRODUCTION

MEASUREMENTS of fast-neutron capture cross sections have proved useful in the determination of the reaction mechanism, individual-level parameters, and average-level properties. These cross sections are also of interest in astrophysical theories of element formation and in reactor design. Application of the Hauser-Feshbach statistical theory<sup>1</sup> to the case of neutron capture<sup>2</sup> enables one to predict capture cross sections averaged over many resonances for reactions proceeding via compound nucleus formation. Several comparisons<sup>2-6</sup> of experimental results with this theory have been made. However, in the mass region near 64 nucleons there are few measurements of neutron capture by nuclides of even mass number in the energy range investigated here. The experiment described here consisted of a measurement of the neutron capture cross section of Ni<sup>64</sup> as a function of energy between approximately 0.2 and 2.0 MeV.

## EXPERIMENTAL TECHNIQUES

Neutrons were produced by means of the Li<sup>7</sup>(*p,n*)Be<sup>7</sup> reaction for neutron energies up to and including 1.205 MeV and the H<sup>3</sup>(*p,n*)He<sup>3</sup> reaction above 1.205 MeV with the Lockheed 3.5-MeV Van de Graaff generator. The lithium targets of 30 to 150 keV thickness at the reaction threshold were made by evaporation of lithium metal onto a 0.005-in.-thick tantalum backing. The evaporations were carried out within the accelerator beam tube onto a target assembly which wobbled to help insure a uniform coating. During proton bombardment the target was also wobbled in order that higher beam currents could be used. For the H<sup>3</sup>(*p,n*)He<sup>3</sup> reaction a tritiated zirconium target on a 0.005-in.-thick platinum backing was used. The platinum backing was

in turn mounted on a 0.005-in.-thick tantalum backing. This target was about 40 keV thick at the reaction threshold.

The neutron capture cross section of Ni<sup>64</sup> was obtained relative to the Au<sup>197</sup>(*n,γ*)Au<sup>198</sup> cross section by activation techniques. Nickel metal chips, enriched to 96.4% in Ni<sup>64</sup>, were contained in a cylindrical plastic holder having 0.015-in.-thick flat faces and a 0.030-in.-thick side. The nickel occupied a volume  $\frac{1}{2}$  in. in diameter by  $\frac{1}{32}$  in. thick. The empty holder was found to exhibit no detectable activity when bombarded with thermal or fast neutrons for times and fluxes comparable to those used for the Ni<sup>64</sup> irradiations. The Ni<sup>64</sup> holder was sandwiched between two 0.001-in.-thick gold foils  $\frac{1}{2}$  in. in diameter. During the irradiations this sandwich was positioned approximately 1 in. from the target with the axis of the cylinder along the 0-deg beam line. Typically, an irradiation was 2.5 h long. The neutron flux was monitored by means of a long counter positioned at 0 deg and about 3 m from the target. Time variations of the neutron flux were taken into account in the cross-section calculations using the long-counter count-rate changes. The effect of room-scattered neutrons was investigated by irradiating the Au and Ni<sup>64</sup> at positions farther from the neutron source. These experiments indicated that the effect of scattered neutrons on the calculated Ni<sup>64</sup>(*n,γ*)Ni<sup>65</sup> cross-section values was less than 4%. After the irradiations the Ni<sup>65</sup>  $\gamma$  radiation was counted with a spectrometer consisting of a 4-in.×4-in. NaI(Tl) crystal, a 100-channel pulse-height analyzer, and associated electronic apparatus. The decay rate of each portion of the spectrum was followed and the half-life was found in every case to be consistent with the average of the two most precise published values,<sup>7,8</sup> this average being 2.561 ± 0.004 h. To obtain the relative Ni<sup>65</sup> yield from one neutron energy to the next, the Ni<sup>65</sup> was counted with a flat face of the holder centered on the flat face of the NaI(Tl) crystal housing. The  $\gamma$ -ray spectrum observed in this geometry is shown in Fig. 1. This spectrum was obtained by counting the Ni<sup>65</sup> sample after irradiation by thermal neutrons, and the count rate was several hundred times higher than that produced by the fast-

† This work was supported by the Lockheed Independent Research Program and the U. S. Atomic Energy Commission.

<sup>1</sup> W. Hauser and H. Feshbach, *Phys. Rev.* **87**, 366 (1952).

<sup>2</sup> B. Margolis, *Phys. Rev.* **88**, 327 (1952).

<sup>3</sup> A. M. Lane and J. E. Lynn, *Proc. Phys. Soc. (London)* **A70**, 557 (1957).

<sup>4</sup> E. R. Rae, B. Margolis, and E. S. Troubetzkoy, *Phys. Rev.* **112**, 492 (1958).

<sup>5</sup> C. Mossin-Kotin, B. Margolis, and E. S. Troubetzkoy, *Phys. Rev.* **116**, 937 (1959).

<sup>6</sup> P. E. Nemirovsky and Yu. P. Yelagin, *Nucl. Phys.* **45**, 156 (1963).

<sup>7</sup> L. M. Silver, *Can. J. Phys.* **29**, 59 (1951).

<sup>8</sup> J. E. Cline and R. L. Heath, *Phys. Rev.* **131**, 296 (1963).

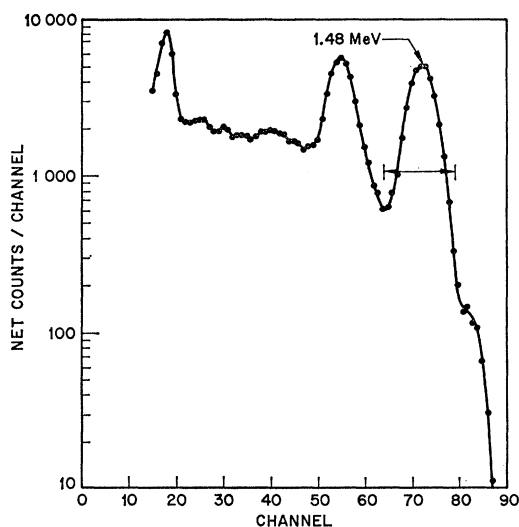


FIG. 1. Gamma-ray spectrum of  $\text{Ni}^{65}$  obtained in close geometry. Horizontal bar indicates portion of spectrum used for relative yield measurements.

neutron irradiations. To obtain the optimum source-to-background-count ratio and to minimize interference from any unknown contaminant activities, only the channel interval (see Fig. 1) which included the 1.48-MeV peak was used for the determination of the relative yield. The gold foils were counted after the nickel in the same geometry. The area under the 412-keV  $\gamma$ -ray peak of  $\text{Hg}^{198}$  was used to obtain the  $\text{Au}^{198}$  yield.

The photopeak efficiency (i.e., the ratio of the counts under a Gaussian curve fitted to a photopeak to the number of  $\gamma$  rays of that energy emitted) had been determined<sup>9</sup> previously in our laboratory for point sources on the crystal axis. Calibrated sources of  $\text{Mn}^{54}$ ,  $\text{Zn}^{65}$ ,  $\text{Na}^{22}$ , and  $\text{Na}^{24}$  obtained from the National Bureau of Standards were counted to determine the efficiency of the crystal as a function of  $\gamma$ -ray energy. In addition, a  $\text{Hg}^{203}$  source calibrated in our laboratory with a  $4\pi$  proportional counter was used. The calibrations of the  $\text{Na}^{22}$  and  $\text{Na}^{24}$  sources were checked by counting the  $\beta$  activity with the  $4\pi$  proportional counter; the agreement was good. From these measurements, the efficiency for the 412-keV  $\gamma$ -ray photopeak relative to the 1.48-MeV peak is believed to be known to within a standard deviation of  $\pm 3\%$ .

The relationship between the count rate in the region encompassing the 1.48-MeV  $\gamma$  ray which was used for relative yield measurements to the actual emission rate of 1.48-MeV  $\gamma$  rays was experimentally studied for the determination of needed corrections. These included: (a) a correction for the counts in the channel interval relative to the counts under a Gaussian curve fitted to the photopeak, (b) the effect produced because the Ni and Au samples were disc sources rather than point sources, (c) the effect of the average source position

being slightly above the crystal can, (d) the effect of self-absorption of the  $\gamma$  rays in the nickel, (e) the effect of absorption of the Ni  $\gamma$  rays by the plastic holder, (f) the effect of  $\beta$  counts included in the channel interval, and (g) subtraction of counts under the 1.48-MeV peak produced by summation of cascade  $\gamma$  rays. None of these corrections was more than 5%. Similar considerations were applied to the  $\text{Au}^{198}$  counts. The average count rate of the two gold foils was used, since this closely represented the average neutron flux over the nickel target.

## RESULTS

The most complete work on the  $\text{Ni}^{65}$  decay scheme has been done by Cline and Heath.<sup>8</sup> They found a value of  $0.25 \pm 0.02$  for the number of 1.48-MeV  $\gamma$  rays per disintegration. This value is in agreement with the work of Siegbahn and Ghosh.<sup>10</sup> The  $\text{Au}^{198}$  decay scheme has been well established.<sup>11</sup> A value of  $0.040 \pm 0.005$  was used for the total internal conversion coefficient of the 412-keV transition and  $99.8_{-0.5}^{+0.2}\%$  was used for the percentage of  $\text{Au}^{198}$  decays proceeding via the 412-keV state in  $\text{Hg}^{198}$ .

Since the  $\text{Ni}^{64}(n,\gamma)\text{Ni}^{65}$  cross sections were found relative to those for the  $\text{Au}^{197}(n,\gamma)\text{Au}^{198}$  reaction, some discussion of the latter is important. In the neutron energy range of interest here the results of various experiments<sup>12</sup> differ by as much as 50% at a given energy, even though the uncertainties quoted for the measurements are only about 10% or less. Most of the recent cross-section work, however, agrees to within about 25%. Gibbons<sup>13</sup> has examined the available cross-section data and has arrived at an estimated best-fit curve of cross section versus energy. That curve has been used in this work. It is estimated by the present author that this curve gives absolute values of the gold cross section accurate to  $\pm 20\%$  in the energy range of interest here. As far as the relative error is concerned, it is estimated that the ratio of the gold cross sections at 0.176 and 1.958 MeV is known to  $\pm 10\%$  and that the relative error is known more accurately within this range depending upon the particular energies considered.

The data were corrected where appropriate for the presence of the second neutron group from the  $\text{Li}^7(p,n)\text{Be}^7$  reaction. The intensity of this group relative to that of the ground-state group was taken from the work of Batchelor.<sup>14</sup> This changed the uncorrected cross sections by 5% at the most.

The average neutron energy was obtained at each energy by numerical integration over the lithium or

<sup>10</sup> K. Siegbahn and A. Ghosh, *Ark. Mat., Astr. Fysik* **36A**, No. 19, (1949).

<sup>11</sup> *Nuclear Data Sheets*, compiled by K. Way *et al.* (Printing and Publishing Office, National Academy of Sciences-National Research Council, Washington, D. C.).

<sup>12</sup> See J. F. Barry, *J. Nucl. Energy A/B18*, 491 (1964), for a recent review of the experiments.

<sup>13</sup> J. H. Gibbons (private communication). Details available from Sigma Center, Brookhaven National Laboratory.

<sup>14</sup> R. Batchelor, *Proc. Phys. Soc. (London)* **A68**, 452 (1955).

<sup>9</sup> J. H. Rowland (private communication).

TABLE I. The Ni<sup>64</sup>(n,γ)Ni<sup>65</sup> activation-cross-section results.

Neutron energy <sup>a</sup> (MeV)	ΔE <sub>n</sub> <sup>b</sup> (MeV)	σ <sub>Au</sub> <sup>c</sup> (mb)	σ <sub>Ni</sub> <sup>d</sup> (mb)
0.176	0.024	286	5.91±1.33
0.190	0.050	281	3.93±0.87
0.273	0.033	252	4.25±1.02
0.368	0.048	206	3.56±0.87
0.458	0.074	171	2.96±0.65
0.533	0.050	153	3.22±0.71
0.635	0.073	132	3.10±0.68
0.738	0.048	115	3.23±0.71
0.819	0.078	106	2.99±0.65
0.935	0.044	98	2.94±0.67
1.036	0.042	94	2.64±0.58
1.109	0.075	92	3.51±0.77
1.205	0.046	90	4.39±1.03
1.359	0.062	87	4.83±1.16
1.502	0.080	82	3.10±0.74
1.654	0.078	77	3.08±0.75
1.795	0.076	69	2.94±0.68
1.958	0.062	62	2.10±0.52

<sup>a</sup> Laboratory system.<sup>b</sup> One-half the full neutron energy spread.<sup>c</sup> The Au<sup>197</sup>(n,γ)Au<sup>198</sup> cross-section values relative to which the Ni<sup>64</sup>(n,γ)Ni<sup>65</sup> cross sections are given.<sup>d</sup> Absolute errors (S.D.) given.

ZrT target thickness and over the angular spread of the nickel-gold sandwich, weighting appropriately to take into account the neutron source reaction angular distributions<sup>15</sup> and the angular variations of nickel or gold thickness seen by the neutrons. The average energy calculated in this way did not vary by more than a few keV from that obtained by a simple average of the minimum and maximum neutron energies on the nickel-gold target.

The relative uncertainties in cross section arise principally from counting statistics ( $\pm 2$ – $12\%$ ) and the uncertainty in the shape of the Au<sup>197</sup>(n,γ)Au<sup>198</sup> cross section ( $\pm 10\%$  at most). The most important factors contributing to the uncertainty in the absolute values of the cross sections but not to relative values are as follows (standard deviations given): (a) relative crystal efficiency for 0.412- and 1.48-MeV γ rays including geometry corrections ( $\pm 3.5\%$ ), (b) decay scheme of Ni<sup>65</sup> ( $\pm 8\%$ ), (c) decay scheme of Au<sup>198</sup> ( $\pm 0.5\%$ ), and (d) Au<sup>197</sup>(n,γ)Au<sup>198</sup> cross-section absolute values. Altogether the absolute values of the Ni<sup>64</sup>(n,γ)Ni<sup>65</sup> cross section are estimated to have uncertainties which are on the average about 23%. These uncertainties, it should be stressed, are based partly upon the estimate stated earlier about the accuracy of the Au<sup>197</sup>(n,γ)Au<sup>198</sup> cross-section curve which was used. When a more definitive knowledge of the gold cross section is obtained, the Ni<sup>64</sup>(n,γ)Ni<sup>65</sup> results given here may be easily renormalized if necessary.

The results are given in Table I and Figs. 2 and 3. Table I gives one-half the full neutron energy spread

<sup>15</sup> *Charged Particle Cross Sections*, edited by N. Jarmie and J. D. Seagrave, Los Alamos Scientific Laboratory Report LA-2014 (Office of Technical Services, U. S. Department of Commerce, Washington, D. C., 1956).

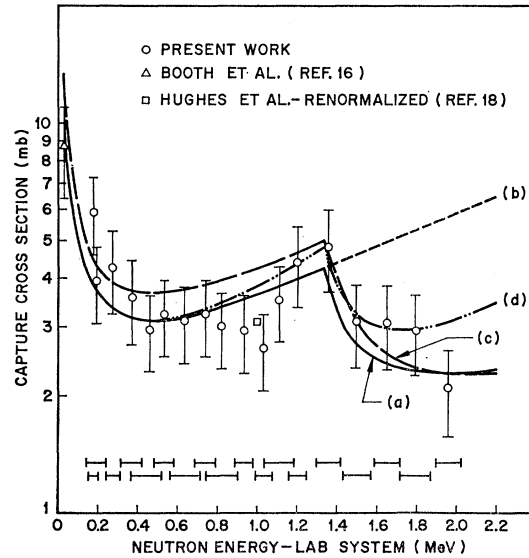


FIG. 2. The Ni<sup>64</sup>(n,γ)Ni<sup>65</sup> cross section. Absolute errors and full neutron energy spreads are shown. Parameters for the theoretical curves are  $\beta=10^{-5}$ ,  $a=10$  MeV<sup>-1</sup>, and  $s/s_R=0.785$ . All curves calculated according to Eq. (1) except that inelastic scattering is neglected for curve (b), the neutron-width-fluctuation correction is ignored for curve (c), and  $T_{\text{rad}}$  instead of  $T_{\text{cap}}$  is used for curve (d).

which is produced by the lithium or zirconium-tritide target thickness and by the kinematical spread from the angle subtended by the Ni<sup>64</sup> target, whereas Figs. 2 and 3 show the full spread by horizontal bars. The Au<sup>197</sup>(n,γ)Au<sup>198</sup> cross section used at each energy is also

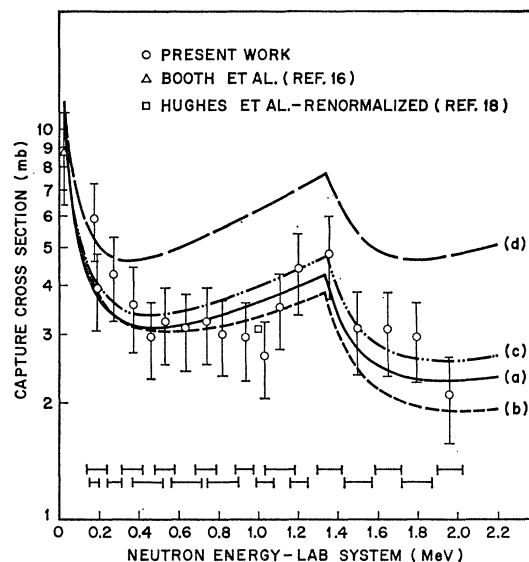


FIG. 3. The Ni<sup>64</sup>(n,γ)Ni<sup>65</sup> cross section. Absolute errors and full neutron energy spreads are shown. All curves are calculated according to Eqs. (1) and (4) with the following parameters: curve (a),  $\beta=10^{-5}$ ,  $a=10$  MeV<sup>-1</sup>,  $s/s_R=0.785$ ; curve (b),  $\beta=10^{-5}$ ,  $a=7.66$  MeV<sup>-1</sup>,  $s/s_R=0.785$ ; curve (c),  $\beta=10^{-5}$ ,  $a=10$  MeV<sup>-1</sup>,  $s/s_R=1$ ; curve (d),  $\beta=10^{-5}$ ,  $a=10$  MeV<sup>-1</sup>,  $s/s_R=\infty$ .

listed in the table. The uncertainties in the absolute  $\text{Ni}^{64}(n,\gamma)\text{Ni}^{65}$  activation-cross-section values are also indicated in Table I and Figs. 2 and 3.

Other work on this cross section has been done with 25-keV neutrons by Booth *et al.*<sup>16</sup> who obtained a value  $8.7 \pm 2.3$  mb and by Kononov *et al.*<sup>17</sup> who got an upper limit of 37 mb. The 8.7-mb value is plotted in Figs. 2 and 3. In addition, Hughes *et al.*<sup>18</sup> measured the cross section with a fission spectrum of neutrons, of effective energy 1 MeV, relative to the thermal cross section and got a value of 5.1 mb. If the more recent thermal-cross-section value<sup>19</sup> of 1.6 b is used instead of the value of 2.6 b which Hughes *et al.* employed, the 1-MeV cross section would be 3.1 mb. It is this renormalized value which is plotted in Figs. 2 and 3. The agreement of this value with the present work is excellent.

## INTERPRETATION

### Summary of Theory

The formalism which was developed by Hauser and Feshbach<sup>1</sup> to interpret fast-neutron inelastic scattering cross sections in terms of the statistical theory of nuclear reactions was extended to the case of fast neutron capture by Margolis<sup>2</sup> and by Lane and Lynn.<sup>3</sup> Several authors<sup>2-6</sup> have subsequently used this theory to compare with observed fast-neutron capture cross sections. The expression for the capture cross section of neutrons whose center-of-mass energy is  $E$  and whose corresponding wave number is  $k$  is the following:

$$\sigma_{\text{cap}}(E) = \frac{1}{2(2I+1)} \frac{\pi}{k^2} \sum_{l=0}^{\infty} \sum_{j=|l-1/2|}^{l+1/2} T_n(lj, E) \times \sum_{J=j-I}^{j+I} \left[ \frac{(2J+1)T_{\text{cap}}(J, E)\mathcal{R}}{T_{\text{rad}}(J, E) + \sum_{E', \nu, j'} T_n(j', E')} \right]. \quad (1)$$

In this formula  $I$  is the target ground-state spin and  $l$  is the orbital angular momentum of the incident neutron. The neutron transmission coefficients  $T_n(lj, E)$  are derived from the optical model with spin-orbit force and therefore depend upon whether the neutron spin vector is parallel ( $j=l+\frac{1}{2}$ ) or antiparallel ( $j=|l-\frac{1}{2}|$ ) with respect to the orbital angular-momentum vector. The neutron transmission coefficients in the denominator refer to all permissible outgoing neutron channels from the compound states having spin  $J$  and having parity which is determined by

<sup>16</sup> R. Booth, W. P. Ball, and M. H. MacGregor, *Phys. Rev.* **112**, 226 (1958).

<sup>17</sup> V. N. Kononov, Iu. Ia. Stavisskii, and V. A. Tolstikov, *Atomnaya Energiya* **5**, 564 (1958) [English transl.: *Soviet J. At. Energy* **5**, 1483 (1958)].

<sup>18</sup> D. J. Hughes, R. C. Garth, and J. S. Levin, *Phys. Rev.* **91**, 1423 (1953).

<sup>19</sup> *Neutron Cross Sections*, compiled by D. J. Hughes and R. B. Schwartz, Brookhaven National Laboratory Report BNL-325, 2nd edition (Superintendent of Documents, U. S. Government Printing Office, Washington, D. C., 1958).

the parity of the target nucleus ground state and by the  $l$  value. Previous authors<sup>3,4,6</sup> have written a corresponding formula in channel-spin notation. The quantity  $T_{\text{rad}}(J, E)$  represents the probability of decay of the compound states of spin  $J$  and given parity by  $\gamma$  emission and is defined in the following way:

$$T_{\text{rad}}(J, E) = \frac{2\pi \langle \Gamma_{\text{rad}}(J, B+E) \rangle}{\langle D(J, B+E) \rangle}.$$

Here  $B$  is the neutron binding energy. If one assumes that the transitions are of the single-particle electric-dipole type and that the levels are closely spaced, this quantity can be approximated<sup>20</sup> by

$$T_{\text{rad}}(J, E) \approx \text{const} \int_0^{B+E} \epsilon^3 \rho(J, B+E-\epsilon) d\epsilon. \quad (2)$$

The integral is taken over all  $\gamma$ -ray de-excitation modes of the original compound states. The quantity  $\rho(J, B+E-\epsilon)$  is the density of all levels which can be reached by electric-dipole transitions of energy  $\epsilon$  from the initial state of spin  $J$  and given parity. A distinction is made between the average radiation width  $\langle \Gamma_{\text{rad}}(J, B+E) \rangle$  and the average capture width  $\langle \Gamma_{\text{cap}}(J, B+E) \rangle$ . If the initial  $\gamma$ -ray transition leaves the compound nucleus in a state whose energy is above the neutron binding energy, then neutron emission will most probably occur and these transitions will not be detected by activation techniques. In that case

$$T_{\text{cap}}(J, E) \equiv \frac{2\pi \langle \Gamma_{\text{cap}}(J, B+E) \rangle}{\langle D(J, B+E) \rangle} \approx \text{const} \times \int_E^{B+E} \epsilon^3 \rho(J, B+E-\epsilon) d\epsilon. \quad (3)$$

The neutron-width-fluctuation correction factor<sup>3</sup>  $\mathcal{R}$  in Eq. (1) is used to correct for the fact that the Hauser-Feshbach formula is written in terms of functions of average widths rather than averages of the functions.

The level-spacing formula which was used for the average spacing of levels of spin  $J$  was that of a Fermi-gas nuclear model. Lang<sup>21</sup> has fitted data from a number of experiments which give level spacing information in order to arrive at the value for  $a$  in the level spacing formula whose spin and energy dependence is given by

$$\langle D(J, B+E) \rangle \propto \frac{\exp[(J+\frac{1}{2})^2/2c\tau] \tau^{3/2}(U+l)^{5/4}}{2J+1 \exp[2(aU)^{1/2}]}. \quad (4)$$

In this formula  $U$  is the excitation energy ( $B+E$ ) minus the pairing energy  $P$  for the particular nucleus involved,  $c$  is a quantity related to the nuclear moment

<sup>20</sup> J. M. Blatt and V. F. Weisskopf, *Theoretical Nuclear Physics* (John Wiley & Sons, Inc., New York, 1952).

<sup>21</sup> D. W. Lang, *Nucl. Phys.* **26**, 434 (1961).

of inertia by  $\mathcal{J} = c\hbar^2$ ,  $\tau$  is the nuclear temperature, and  $t$  is the thermodynamic temperature. The nuclear equation of state is

$$U = at^2 - t$$

and  $\tau$  is related to  $a$  through the expression

$$a = U/\tau^2 + 2.5/\tau.$$

Lang used the shell model work of Jensen and Luttinger<sup>22</sup> to arrive at the value for  $c$ , which in terms of  $a$  and the mass  $A$  is

$$c \approx 0.0888aA^{2/3}. \quad (5)$$

Lang, following a form chosen by Newton<sup>23</sup> but re-evaluating the constant, found that the shell structure of the level density could be displayed by using the following expression to fit the values of  $a$  derived from experiments:

$$a = 0.0748(\bar{j}_n + \bar{j}_p + 1)A^{2/3}. \quad (6)$$

Here,  $\bar{j}_n$  and  $\bar{j}_p$  are the effective values of the total angular momentum for the neutrons and protons, respectively, according to the shell model for the particular nucleus. Tables of  $(2\bar{j}_n + 1)$  and  $(2\bar{j}_p + 1)$  are given by Newton.

#### Application of Theory to Ni<sup>64</sup>( $n, \gamma$ )Ni<sup>65</sup> Cross Section

The ground-state spin and parity of Ni<sup>64</sup> is 0+ while that of the first excited state at 1.34 MeV is 2+. From the nuclear systematics the second excited state would be expected to be at approximately 2 MeV. The second excited state is not included in the theoretical calculations given here. The spin-0 ground state simplifies Eq. (1) since the summation over  $J$  includes only  $J = j$ .

Instead of using the constant itself in Eqs. (2) and (3) as a parameter, the quantity  $\beta = \langle \Gamma_{\text{rad}}(\frac{1}{2}, B) \rangle / \langle D(\frac{1}{2}, B) \rangle$  was used. This then could be compared with measurements in the resonance region if they exist. Note that for  $J = \frac{1}{2}$ , since only states of spin  $\frac{1}{2}$  and  $\frac{3}{2}$  can be populated by electric dipole emission,

$$\rho(\frac{1}{2}, B + E - \epsilon) = \langle D(\frac{1}{2}, B + E - \epsilon) \rangle^{-1} + \langle D(\frac{3}{2}, B + E - \epsilon) \rangle^{-1},$$

whereas for  $J > \frac{1}{2}$  the sum includes three terms ( $J - 1$ ,  $J$ , and  $J + 1$ ). Use is made of the facts that the density of states of a given spin and parity is the inverse of their spacing and that the densities of various spin states are added to get the total density. In evaluating the expressions for  $T_{\text{rad}}$  and  $T_{\text{cap}}$  the  $J$ -dependent parts of  $\rho(J, B + E - \epsilon)$  were taken outside the integral with  $\tau$  in the factor  $2c\tau$  evaluated at the energy corresponding to the value of  $\epsilon$  midway between the limits of integration. For Ni<sup>64</sup>,  $B = 6.14$  MeV.<sup>11</sup> Although the Fermi-gas level-spacing formula is not expected to be accurate at low excitation energies, it was used all the

way to  $U = 0$ . Because of the pairing energy correction,  $U = 0$  corresponds to an actual excitation energy  $P$ . For  $U < 0$  the spacing was taken to be that at  $U = 0$ . The pairing energy for Ni<sup>65</sup> is 1.41 MeV according to the work of Stolovy and Harvey.<sup>24</sup>

The correction factors  $\mathcal{R}$  for neutron capture were evaluated according to the formula and procedure given by Moldauer,<sup>25</sup> with the substitutions  $\langle \tau_c \rangle \rightarrow T_n$  and  $\langle \tau_\gamma \rangle \rightarrow T_{\text{rad}}$  in his formula. The neutron widths were assumed to follow a Porter-Thomas distribution and the radiation widths were assumed to be constant from resonance to resonance of the same spin at a given excitation energy.

Although experimental level-density information on Ni<sup>65</sup> itself is lacking, the work of Lang<sup>21</sup> on extracting this information for neighboring nuclei would suggest the value  $a \approx 10$  MeV<sup>-1</sup> in the level-spacing formula [Eq. (4)] for  $A = 65$ . The expression Eq. (6), which was used by Lang to provide an over-all fit to the available experimental information for all values of  $A$ , gives  $a = 7.66$  MeV<sup>-1</sup> for Ni<sup>65</sup>.

Figure 2, curve (a) shows a theoretical fit to the observed Ni<sup>64</sup>( $n, \gamma$ )Ni<sup>65</sup> cross sections, using Eq. (1). Here the value  $a = 10$  MeV<sup>-1</sup> was used. The constant  $c$  in the  $J$ -dependent part of the level spacing formula was taken from Eq. (5) and corresponds to a moment of inertia which is 0.785 that of the rigid-body value<sup>26</sup>  $\mathcal{J}_R = \frac{2}{5}MR^2A$ , where the latter is computed using a nuclear radius  $R = 1.2A^{1/3}$  F and  $M$  is the nucleon mass. Transmission coefficients were used which were calculated with the ABACUS program of Auerbach<sup>27</sup> from the optical-model parameters of Moldauer<sup>28</sup> [see Eq. (8) in Ref. 28 for the parameters used]. Moldauer obtained his parameters by fitting the primary neutron data of  $s$ -wave neutron strength functions, total cross sections up to 1 MeV, and elastic scattering cross sections up to the inelastic threshold energies for nuclei in this mass range. It was found, for example, that the results of curve (a) were 13% lower at 25 keV, less than 1% different between 0.1 and 1.3 MeV, and 10% lower at 2 MeV if the transmission coefficients<sup>29</sup> derived from optical model parameters of Perey and Buck<sup>30</sup> were used. The transmission coefficients<sup>29</sup> obtained using the parameters of Bjorklund and Fernbach<sup>31</sup> gave results 10% lower at 25 keV, less than 4% lower between 0.1 and 1.3 MeV, and 10% lower at 2 MeV. This insensitivity to the choice of transmission coefficients occurs because the capture cross section is so small; i.e., for most terms in Eq. (1),  $T_{\text{rad}} \ll T_n$  and these terms (below the inelastic

<sup>24</sup> A. Stolovy and J. A. Harvey, Phys. Rev. **108**, 353 (1957).

<sup>25</sup> P. A. Moldauer, Phys. Rev. **123**, 968 (1961).

<sup>26</sup> C. Bloch, Phys. Rev. **93**, 1094 (1954).

<sup>27</sup> E. H. Auerbach (private communication).

<sup>28</sup> P. A. Moldauer, Nucl. Phys. **47**, 65 (1963).

<sup>29</sup> E. H. Auerbach and F. G. J. Perey, *Optical Model Transmission Coefficients, 0.1 to 5.0 MeV*, Brookhaven National Laboratory Report BNL-765 (Office of Technical Services, Department of Commerce, Washington, D. C., 1962).

<sup>30</sup> F. Perey and B. Buck, Nucl. Phys. **32**, 353 (1962).

<sup>31</sup> F. Bjorklund and S. Fernbach, Phys. Rev. **109**, 1295 (1958).

<sup>22</sup> J. H. D. Jensen and J. M. Luttinger, Phys. Rev. **86**, 907 (1952).

<sup>23</sup> T. D. Newton, Can. J. Phys. **34**, 804 (1956).

threshold) can be approximated in the following way:

$$T_n T_{\text{cap}} / (T_{\text{rad}} + T_n) \approx T_{\text{cap}}. \quad (7)$$

This form is almost independent of  $T_n$ . It can be seen that under this condition the constant  $\beta$  acts simply to normalize the whole cross-section curve. In fact if  $\beta = 0.8 \times 10^{-5}$ , for example, the results of curve (a), Fig. 2, are lowered by 16% at 25 keV, 18% at 1 MeV, and 20% at 2 MeV. The terms contribute to the sum until  $T_n \ll T_{\text{rad}}$ . Because of the small values for  $T_{\text{rad}}$ , terms through  $l=2$  at 25 keV and  $l=5$  at 2.0 MeV contributed appreciably. It was found that more accurate values for  $T_n$  when  $T_n < 10^{-5}$  could be obtained by extrapolating log-log plots of  $T_n(l, E)$  versus energy rather than by taking these small values directly from the ABACUS program. As can be seen on curve (a), the experimental results drop sharply near 1.34 MeV which is where inelastic scattering begins to compete as a compound-nucleus de-excitation mechanism. Neglect of the 1.34-MeV state in the calculations is indicated by curve (b) in Fig. 2; inclusion of this state is clearly necessary in this theory to produce the desired dropoff. Also indicated in Fig. 2 as curve (c) is the effect obtained by neglecting the neutron-width-fluctuation effect, i.e., letting all  $\mathcal{R}=1$ . At the lower energies these factors lower the uncorrected cross sections by about 20%; well above the inelastic threshold, the effect is reversed and the uncorrected results are lower. Curve (d) shown in Fig. 2 corresponds to the cross sections obtained when  $T_{\text{rad}}$  instead of  $T_{\text{cap}}$  is used in the numerator of Eq. (1). The neutron-width-fluctuation correction is included. This change is quite significant at the higher energies; for example, the cross-section values at 2 MeV are increased by about 40%. The value  $\beta = 10^{-5}$  was chosen because it provided a fairly good over-all fit for the fully corrected results. In addition the fit is within the error bar at the 25-keV point where, it will be seen, adjustments in the various parameters have the least effect. As mentioned earlier, below an excitation energy of 1.41 MeV the level spacing was taken to be the same as that at 1.41 MeV. If transitions to states below 1.41 MeV were neglected altogether, the cross sections of curve (a) would be increased by less than 1% at 25 keV, by 5% at 1 MeV, and by 8% at 2 MeV.

Figure 3 indicates the effect of varying the parameter  $a$  in the level-spacing formula. Curve (a) in Fig. 3 is the

same as curve (a) in Fig. 2. Curve (b) in Fig. 3 arises by changing  $a$  to  $7.66 \text{ MeV}^{-1}$ , leaving the other parameters fixed. It is seen that at the lower energies the two curves are essentially identical but at the higher energies curve (a) may represent a somewhat better fit to the data. As indicated in curve (c) in Fig. 3 the cross-section values of curve (a) are raised by less than 15% by changing only the parameter  $c$  in the set corresponding to curve (a) to a value equal to the rigid-body value. On the other hand if  $c = \infty$ , corresponding to a simple  $(2J+1)^{-1}$  dependence of the level spacing, the curve is raised by almost a factor of 2 at the highest energy shown but by only about 10% at 25 keV. This is shown in curve (d), Fig. 3. However, a renormalization by changing  $\beta$  could still produce a rather good fit to the data.

From total-neutron cross-section measurements on  $\text{Ni}^{64}$  between 10 and 600 keV, Farrell *et al.*<sup>32</sup> determined an average  $s$ -wave level spacing of about 24 keV. Taking this to be the spacing at 305 keV, Eq. (4) gives a spacing of about 34 keV at the neutron binding energy for the  $\frac{1}{2}+$  levels. This result together with the value  $\beta = 10^{-5}$  suggests an average radiation width  $\langle \Gamma_{\text{rad}}(\frac{1}{2}, B) \rangle = 0.34 \text{ eV}$ . This value is consistent with more direct measurements<sup>24,33</sup> of radiation widths made in this mass region.

In conclusion, the statistical theory of nuclear reactions, together with the Fermi-gas level-spacing formula, gives a good fit to the  $\text{Ni}^{64}(n, \gamma)\text{Ni}^{65}$  cross-section data. A straightforward application of the theory with parameters taken from the results of other work leaves only one free parameter,  $\beta$ . The value of this parameter together with the measured spacing of  $s$ -wave resonances serves as a determination of the radiation width of  $\frac{1}{2}+$  levels at the neutron binding energy.

#### ACKNOWLEDGMENTS

The author wishes to acknowledge the help of Dr. R. G. Johnson for suggesting this measurement and Dr. W. L. Imhof and Dr. F. J. Vaughn for their preliminary experiments. In addition the assistance of H. O. Menlove in the data reduction and K. L. Coop in the theoretical calculations is greatly appreciated.

<sup>32</sup> J. A. Farrell, E. G. Bilpuch, and H. W. Newson (unpublished).

<sup>33</sup> J. S. Levin and D. J. Hughes, *Phys. Rev.* **101**, 1328 (1956).